CHIN. PHYS. LETT. Vol. 38, No. 11 (2021) 116802 **Express Letter**

Unexpected Selective Absorption of Lithium in Thermally Reduced Graphene Oxide Membranes

Jie Jiang(江杰)[1,2†], Liuhua Mu(木留华)[1,2†], Yu Qiang(强羽)[3†], Yizhou Yang(杨一舟)[3], Zhikun Wang(王志坤)[4], Ruobing Yi(伊若冰)[1,2], Yinwei Qiu(裘银伟)[4], Liang Chen(陈亮)[4*], Long Yan(闫隆)[1*], and Haiping Fang(方海平)[1,3*]

[1]*Shanghai Institute of Applied Physics, Chinese Academy of Sciences, Shanghai 201800, China*
[2]*University of Chinese Academy of Sciences, Beijing 100049, China*
[3]*Department of Physics, East China University of Science and Technology, Shanghai 200237, China*
[4]*Department of Optical Engineering, Zhejiang Provincial Key Laboratory of Chemical Utilization of Forestry Biomass, Zhejiang A&F University, Hangzhou 311300, China*

(Received 29 September 2021; accepted 25 October 2021; published online 27 October 2021)

Lithium plays an increasingly important role in scientific and industrial processes, and it is extremely important to extract lithium from a high Mg^{2+}/Li^{+} mass ratio brine or to recover lithium from the leachate of spent lithium-ion batteries. Conventional wisdom shows that Li^{+} with low valence states has a much weaker adsorption (and absorption energy) with graphene than multivalent ions such as Mg^{2+}. Here, we show the selective adsorption of Li^{+} in thermally reduced graphene oxide (rGO) membranes over other metal ions such as Mg^{2+}, Co^{2+}, Mn^{2+}, Ni^{2+}, or Fe^{2+}. Interestingly, the adsorption strength of Li^{+} reaches up to 5 times the adsorption strength of Mg^{2+}, and the mass ratio of a mixed Mg^{2+}/Li^{+} solution at a very high value of 500 : 1 can be effectively reduced to 0.7 : 1 within only six experimental treatment cycles, demonstrating the excellent applicability of the rGO membranes in the Mg^{2+}/Li^{+} separation. A theoretical analysis indicates that this unexpected selectivity is attributed to the competition between cation–π interaction and steric exclusion when hydrated cations enter the confined space of the rGO membranes.

DOI: 10.1088/0256-307X/38/11/116802

Lithium plays an increasingly important role in scientific and industrial processes, e.g., used for storage equipment,[1−3] lithium-ion batteries (LIBs),[4,5] alloy technology,[6,7] glass,[8] and ceramics,[9] resulting in a rapidly growing demand for lithium resources from extraction and recovery.[10−14] Almost 60% of the world's lithium is contained in salt lake brines, which are regarded as the primary source of lithium.[15] Spent lithium-ion batteries are considered to be a secondary source of lithium.[12] Various traditional separation methods have been used to extract lithium from brines and recover lithium from the leachate of spent LIBs, including precipitation,[16] solvent extraction,[17] crystallization[18] and ion exchange.[15] However, effectively separating lithium from brine[16,17,19] or leachate containing multiple coexisting ions[12,20,21] is still a great challenge because of their similar ionic properties. For example, many salt lake brines have a high Mg^{2+}/Li^{+} mass ratio (from 35 : 1 to 1837 : 1),[19] and this high mass ratio and the corresponding low concentrations of Li^{+} significantly limit the extraction of lithium from brines.[19,22] Further, conventional methods for the recovery of lithium from leachate are usually followed by solvent extraction or precipitation, which leads to serious loss of lithium.[18,23] Thus, these conventional technologies for lithium extraction and recovery are either expensive to operate, time consuming, low efficiency, or high cost[10,11] and will struggle to meet future demand.

Adsorption separation technology is an important chemical separation method for high efficiency extraction, concentration, and purification. Due to the cation–π interactions,[24,25] it is found that both Li^{+} and Mg^{2+} can be strongly absorbed on the aromatic rings structure in graphene-based materials. Conventional wisdom is that Li^{+} has a low valence state so that it has a much weaker adsorption energy with the graphene than multivalent ions. Therefore, we do not expect that Li^{+} has the selective adsorption over other metal ions such as Mg^{2+}, Co^{2+}, Mn^{2+}, Ni^{2+}, or Fe^{2+} in thermally reduced graphene oxide (rGO) membranes.[26]

In this work, we experimentally show that Li^{+} has the selective adsorption over other metal ions such as Mg^{2+}, Co^{2+}, Mn^{2+}, Ni^{2+}, or Fe^{2+} in thermally rGO membranes, and the adsorption strength of Li^{+} reaches up to 5 times the adsorption strength of Mg^{2+}. The findings provide a new way to extract and recover lithium, which has the potential to contribute to sustainable lithium supplies for batteries and su-

Supported by the Fundamental Research Funds for the Central Universities, the National Natural Science Foundation of China (Grant Nos. 11974366, 11675246, 12074341, U1832170, and U1832150), the Key Research Program of Chinese Academy of Sciences (Grant No. QYZDJ-SSW-SLH053), the Computer Network Information Center of the Chinese Academy of Sciences, and the Shanghai Supercomputer Center of China.
†These authors contributed equally to this work.
*Corresponding authors. Email: fanghaiping@sinap.ac.cn; yanlong@sinap.ac.cn; liangchen@zafu.edu.cn
© 2021 Chinese Physical Society and IOP Publishing Ltd

percapacitors and the development of lithium-based technologies in various fields, such as the automotive, aerospace, and metallurgical industries.

Results and Discussion—High Li^+ Selectivity of rGO Membranes in Mixed Salt Solutions. Freestanding graphene oxide (GO) membranes[27–30] were prepared from natural graphite powders via a modified Hummer method as described previously. These GO membranes were treated at 140 ℃ for one hour, and the resulted membranes are denoted as dried rGO-140. These dried rGO-140 membranes were then immersed in a series of $LiCl + MCl_2$ mixed solutions (where M = Mg^{2+}, Ni^{2+}, Co^{2+}, Fe^{2+}, or Mn^{2+}) at room temperature for one hour. The initial molar ratios in the mixed solutions (denoted R_i) for M:Li^+ were R_i = 150 : 1 (3 mol/L M and 0.02 mol/L Li^+) and 1 : 1 (1 mol/L M + Li^+), respectively. We refer to the resulted membranes as wet rGO-140 membranes. These wet rGO-140 membranes, now saturated with salt solution, were removed from the solution and desorbed with 1 mmol/L HCl, and the metal ions in the wet rGO-140 membranes were determined by inductively coupled plasma optical emission spectroscopy (ICP-OES, see details in the Supplementary Material) after removal of the solution on the surface. Then, we obtained the M/Li^+ molar ratios in the wet rGO-140 membranes (denoted R_f) and R_f/R_i. Figure 1(c) shows that R_f/R_i is 0.21, 0.17, 0.19, 0.20, and 0.22 for M = Mg^{2+}, Ni^{2+}, Co^{2+}, Fe^{2+}, or Mn^{2+}, respectively. Furthermore, we performed experiments on the initial mixed solution with R_i = 1 : 1 and found that R_f/R_i was 0.45, 0.43, 0.42, 0.44, and 0.47, respectively [inset in Fig. 1(c)]. The molar ratios of M/Li^+ in the wet rGO-140 membranes are about five and two times higher than the initial molar ratios of 150 : 1 and 1 : 1, respectively. Thus, the rGO membranes show good selective adsorption for Li^+ ions over the other metal ions.

Li^+ Selectivity in a Mixed Mg^{2+}/Li^+ Solution with a Very High Mass Ratio. Based on this selective adsorption behavior, the mass ratio of a mixed Mg^{2+}/Li^+ solution with a very high value can be effectively reduced to a low value with several treatment cycles. Immersion of the rGO membranes in an initial mixed salt solution to selectively adsorb and separate the lithium was considered to compose a treatment cycle. In the experiment, the initial Mg^{2+}/Li^+ ratio of the salt solution in the next cycle was set to be the Mg^{2+}/Li^+ ratio of the output salt solution in the previous cycle. As shown in Fig. 1(d), starting from a very high value of 500 : 1, the mass ratio after six cycles was about 3 orders of magnitude lower than that of the initial mixed Mg^{2+}/Li^+ solution, reaching 0.7 : 1. Here, we use the mass ratio as the unit because it is more commonly used in the industry. Note that excellent selective-separation performance of the rGO-140 membranes was observed for the solutions with a wide range of initial mass ratios [500 : 1–1.2 : 1 in Fig. 1(d)]. This range encompasses the mass ratios of many salt lakes. Furthermore, R_f in the last cycle was 0.2 : 1 (0.7 : 1 as the mass ratio) after six treatment cycles, which shows that the moles of Li^+ aggregated in the wet rGO-140 membranes were about five times higher than those of Mg^{2+}. These observation results indicate that lithium ions can be effectively enriched through these rGO-140 membrane treatment processes.

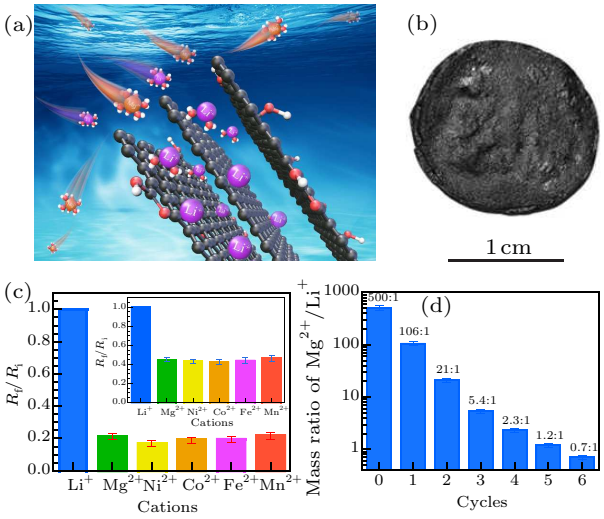

Fig. 1. Effectively separating Li^+ ions from other metal ions using rGO-140 membranes. (a) A schematic of separation of Li^+ ions by rGO-140 membranes. (b) Photograph of a freestanding rGO membrane prepared by drop-casting of a 5 mg/mL graphene oxide suspension. (c) Ratios between the M/Li^+ molar ratios in the wet rGO-140 membranes (R_f) and those in the initial solutions (R_i). These wet rGO-140 membranes were immersed in various salt solutions with R_i = 150 : 1 and 1 : 1 (inset), respectively. (d) Mass ratio with respect to the treatment cycles by rGO-140 membranes. Error bars indicate the standard deviation.

Efficiency of Selective Separation for Different rGO Membranes. The preparation of suitable rGO membranes, particularly the reduction temperature used in the heat treatment, is of crucial importance for the efficiency of selective separation. Figure 2(a) shows the dependence of R_f/R_i on the reduction temperature. Here, R_i was 1 : 1 for the salt solution with a concentration of 1 mol/L. It is clear that, upon increasing the reduction temperature from 100 ℃ to 140 ℃, R_f/R_i significantly decreased from 1.02 to 0.45. Then, R_f/R_i increased to 0.60 as the reduction temperature further increased from 140 ℃ to 170 ℃, and it slightly decreased at 180 ℃. Interestingly, the dependence of the adsorption capacity of cations on the reduction temperature is quite similar to that of R_f/R_i (see Fig. S1 in the Supplementary Material). Thus, rGO-140 has the best performance in terms of selectivity. The membranes reduced at lower temperatures (100–120 ℃), denoted as rGO-(100–120), can absorb more ions and have a relatively lower selectivity for Li^+, while the membranes reduced at higher temperatures (140–180 ℃), denoted as rGO-(140–180), can absorb relatively fewer ions and have a higher selec-

tivity for Li^+ over Mg^{2+}.

Interlayer Spacings of Selective Separation for Different rGO Membranes. We used x-ray diffraction (XRD) to analyze the rGO membranes obtained with different reduction temperatures. The interlayer spacings (denoted as d) of the rGO membranes were indicated by the Bragg peaks in the XRD spectrum. There appear peaks at 11.6° and 12.6°, indicating that d was 7.6 Å and 7.0 Å for the dried rGO-100 and rGO-120 membranes, respectively, as shown in Fig. 2(b). All the dried rGO-(140–180) membranes have peaks at 24.3°, corresponding to a d value of 3.7 Å. These dried rGO membranes were then immersed in salt solutions with $R_i = 1:1$ and analyzed by XRD. As shown in Fig. 2(c), the wet rGO-100 and rGO-120 membranes had peaks that moved to 6.7° and 7.2°, indicating values of d of 13.0 Å and 11.8 Å, respectively, and the peaks located at 24.3° for all the wet rGO-(140–180) membranes, showing the same value of d at 3.7 Å. Clearly, for the reduction temperature <140 ℃, the interlayer spacings of the dried rGO-(100–120) membranes only allowed one single water molecule or monolayer to stay, and the wet rGO-(100–120) membranes had wide interlayer spacings (11.8–13.0 Å) that were accustomed to fully hydrated ions, according to earlier reports.[31–33] Importantly, for a reduction temperature ≥140 ℃, the rGO-(140–180) membranes have narrow interlayer spacings of 3.7 Å in both dry and wet states, which only allow the ions to stay in partially or fully dehydrated states.

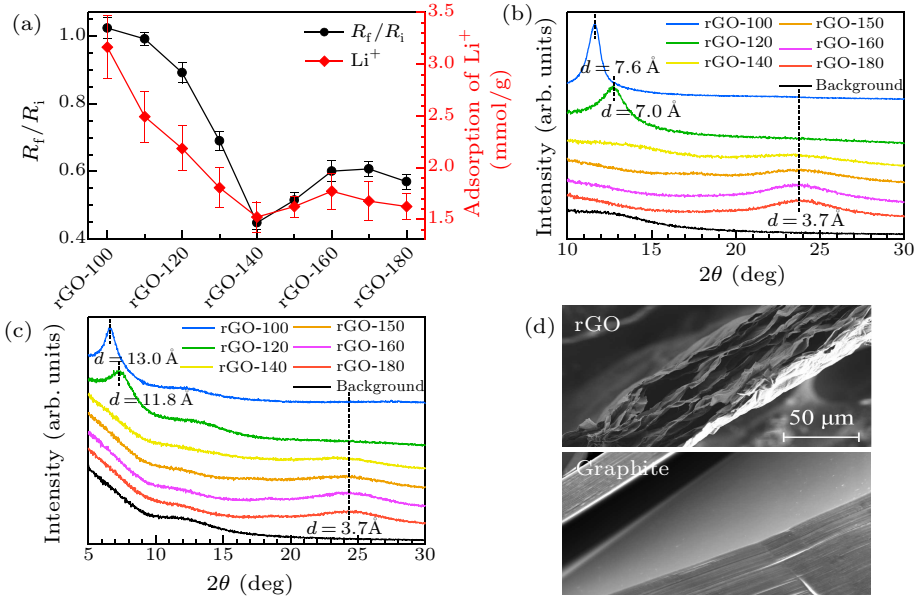

Fig. 2. Selective-separation performances of rGO membranes at different reduction temperatures. (a) Effect of reduction temperature on R_f/R_i for $R_i = 1:1$ (black circles). The adsorption capacity of rGO membranes for Li^+, which are immersed in salt solutions with $R_i = 1:1$ (red diamonds). Corresponding membranes are denoted as rGO-temperature, and the temperature was used in heat treatment. (b) XRD patterns of the rGO membranes reduced at various temperatures. (c) XRD patterns of the rGO membranes reduced at various temperatures and then immersed in salt solutions with $R_i = 1:1$. (d) SEM images of parts of the rGO-140 membrane and graphite. Error bars indicate the standard deviation.

Mechanism of Selectivity Behavior. We performed density functional theory (DFT) calculations to explore the underlying physics. As revealed by the XRD analyses, both the dried and wet rGO-(140–180) membranes have peaks at 24.3°, indicating the interlayer spacing of 3.7 Å. Clearly, ions can stay in their partially or fully dehydrated states. Therefore, in the following, we exploited the energy barriers for the fully dehydrated cation intercalation into the space between two neighboring graphene sheets with the interlayer spacing (denoted as d) of 3.7 Å and defined the energy barriers (ΔE^D) as

$$\Delta E^D(d) = E_f^{D\text{-}C}(d) - E_i^{H\text{-}C}(d), \quad (1)$$

where $E_f^{D\text{-}C}(d)$ denotes the total energies of the dehydrated cation (denoted D-C, C = Li^+ or Mg^{2+}) intercalation into the space between two neighboring graphene sheets with a narrow interlayer spacing of $d = 3.7$ Å, and $E_i^{H\text{-}C}(d)$ represents the total energies of the hydrated cation (denoted H-C, C = Li^+ or Mg^{2+}) adsorbed onto two neighboring graphene sheets with a narrow interlayer spacing of $d = 3.7$ Å. We optimized the geometries of the hydrated cations adsorbed on two neighboring graphene sheets and the geometries of the dehydrated cation intercalation into the space between two neighboring graphene sheets, where the neighboring graphene sheets all have a narrow interlayer spacing of $d = 3.7$ Å, as shown in Fig. 3(a). Figure 3(b) shows that the energy barrier of dehydrated Li^+ (40.71 kcal/mol) is significantly lower than the energy barrier of dehydrated Mg^{2+} (110.73 kcal/mol), indicating that the dehydrated Li^+ enters the narrow interlayer spacing much more easily than dehydrated Mg^{2+}.

Clearly, such high selectivity of Li^+ results from the competition between cation–π interaction and steric exclusion. Hydrated Li^+ and Mg^{2+} ions can be strongly absorbed on the graphene due to the cation–π interactions. Conventional wisdom shows that Li^+ with low valence states has a much weaker absorption energy with graphene than Mg^{2+}. However, Li^+ has a smaller energy barrier so it is easier to dehydrate and enter the confined spacing. Here, the rGO-(140–180) membranes have much smaller interlayer spacing as the confined spacing and are accustomed to dehydrated ions. The membranes exclude hydrated Mg^{2+} that require a larger interlayer spacing, and allow dehydrated Li^+ with smaller sizes to be adsorbed in, and this yields an unexpected high selective adsorption for Li^+, consistent with our experimental observation in Fig. 2(a).

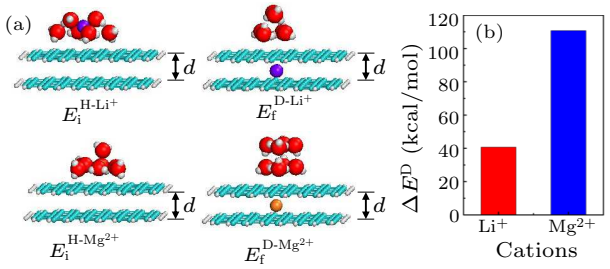

Fig. 3. Theoretical computations for dehydrated or hydrated cation intercalation into the space between two neighboring graphene sheets. (a) The most stable optimized geometries of hydrated/dehydrated Li^+ and Mg^{2+} interacting with two neighboring graphene sheets from a density functional theory computation, where the neighboring graphene sheets have a fixed interlayer spacing of $d = 3.7$ Å for both $E_i^{H\text{-}C}$ and $E_f^{D\text{-}C}$. (b) Energy barriers for dehydrated Li^+ and Mg^{2+} to intercalate into the space between two neighboring graphene sheets. Spheres in purple, orange, cyan, white, and red represent Li^+, Mg^{2+}, carbon, hydrogen, and oxygen, respectively.

Previous theoretical studies have shown that Li^+ can reversibly intercalated into natural graphite with small energy cost.[34–37] However, to the best of our knowledge, there is no experimental report on the massive intercalation of Li^+ into natural graphite. We think that the defects, wrinkles, and edges of the graphene layers allow Li^+ ions to massively and rapidly intercalate into the rGO membranes. The existence of those defects, wrinkles, and edges has been demonstrated by Raman spectra (see Fig. S2 in the Supplementary Material) and scanning electron microscope (SEM) images [see Fig. 2(d)]. Clearly, the defects, wrinkles, and edges of the graphene layers will make other ions, including Mg^{2+} ions, intercalate into the rGO membranes much easier, whereas the different energy barriers for the intercalation will result in the selective adsorption and separation behavior.

In summary, we have experimentally shown that rGO membranes have good selective adsorption for Li^+ ions over other metal ions M (M = Mg^{2+}, Ni^{2+}, Co^{2+}, Fe^{2+}, or Mn^{2+}) in mixed salt solutions with a high mass ratio of M/Li^+. More importantly, lithium ions can be effectively enriched within six treatment cycles by these rGO membranes reduced at temperature of 140 ℃, which shows great potential for use in the extraction of lithium from brines or in the recovery of lithium from spent LIBs. Our computations indicate that due to the competition between cation–π interaction and steric exclusion, dehydrated Li^+ can enter the narrower interlayer spacing and absorbed into the confined spacing much more easily than dehydrated Mg^{2+}, yielding the higher selective adsorption for Li^+. Certainly, the ions absorbed in the rGO membranes can be desorbed so that the rGO membranes can be reused (see the Supplementary Material).

Finally, we would like to say that the rGO membranes reduced at different temperatures can also be applied to the separation of other ions by considering the match between the interlayer spacings and the sizes of the ions. Thus, these findings represent a step towards sustainable sources of lithium and other metals for various applications.

Material and Methods—Freestanding GO and rGO Membranes Preparation. Graphene oxide (GO) was prepared from natural graphite powder via a modified Hummers method.[38–40] Graphite powders were put into concentrated H_2SO_4, $K_2S_2O_8$, and P_2O_5 solution and stirred continuously for several hours. Then the mixture was diluted with deionized water (DI), centrifuged, and washed with DI water. After drying, preoxidized graphite was obtained. Then, they were further oxidized in concentrated H_2SO_4 and $KMnO_4$, diluted with DI water, followed by the addition of 30% H_2O_2. The product was centrifuged and washed with 1 : 10 HCl aqueous solution and DI water sequentially to remove ion species. Finally, few-layer graphene oxide was separated by centrifugation at 4000 rpm. The concentration of the as-prepared GO suspension was approximately 5 mg/mL. Freestanding GO membranes could be prepared by drop-casting the GO suspension (5 mg/mL, 1 mL) droplets onto a smooth paper substrate.[41]

In order to speed up the preparation process without affecting the quality of GO membranes, the freestanding GO membranes in our study were drying thoroughly at 60 ℃ for twelves hours. After that, they were peeled off, rinsed and soaked with DI water for more than half an hour to remove the absorbed metal ions, then dried in a dry dish at room temperature for three days. These GO membranes underwent reduction by heat treatment at different temperatures for one hour to obtain the rGO membranes. The prepared GO and rGO membranes were stored in dry and clean containers before usage.

ICP-OES. The metal ions content in the mixed solution was quantified using a PerkinElmer Optima 7000DV ICP-OES system. The samples were diluted with DI water, and calibration curves were generated using at least 5 ICP standard solutions, with the results used only from correlation coefficients that were

greater than 0.999. The gas nebulizer flow rate range was set between 0.45 and 0.75 L/min, and 1 wavelength per element were used in the radial mode unless otherwise stated: lithium (670.784 nm), magnesium (279.079 nm), cobalt (228.616 nm), iron (259.940 nm), nickel (231.604 nm) and manganese (257.610 nm). The concentrations reported here are the average of three replicates.

XRD. Using 40 kV and 40 mA Cu K_α radiation, a Bruker D8 Advance XRD was used to characterize the structure of the rGO membranes before and after immersing. The rGO membranes placed on a zero-background sample holder. The instrument scan speed was set to 4.5°/min and scanned from 5–90° (2θ).

Scanning Electron Microscopy. On an LEO 1530VP, the rGO membranes were mounted on carbon tape and analyzed using 10 kV with a working distance of 8.3 mm. The dwell time was set to 2 µs, and the images used in this work were magnified at 5000×. No further image processing was performed.

Raman. The Raman spectrometer (Horiba Jobin-Yvon, HR 800) with 1064 nm excitation, an InGaAs detector, and 0.5 W power was used in the experiment. The rGO membranes were placed in a sample holder for Raman measurement. The spectra were collected using 256 scans/sample at resolution of 8 cm^{-1}.

Theoretical Calculation. The Graphene sheet is modeled as $C_{84}H_{24}$, (12.28 × 15.67 $Å^2$, 84 carbon atoms and 24 hydrogen atoms), which is large enough to mimic the graphite surface with a tolerable error.[42] Considering that previous studies have revealed that the hydration shells of Li^+ and Mg^{2+} contain, respectively, 4–6 and 6–8 water molecules,[43–45] we investigated the possible geometries of the Li^+–$(H_2O)_6$@graphene, and Mg^{2+}–$(H_2O)_8$@graphene clusters. All initial structures optimized at the M062X/6-31G(d) level, and the total charge was 1e and 2e for the system containing Li^+ and Mg^{2+}, respectively. We note that the meta-GGA hybrid functional M06-2X[46,47] has been widely used to study the cation–π systems containing cations and aromatic ring structures,[48–51] because it can be used to accurately describe non-covalent interactions in dispersion-dominated complexes and the cation–π interactions.[52] In particular, the geometry optimizations are performed via the Berny algorithm[44,45,53] with the convergence criteria of a maximum step size of 0.0018 a.u. and a root-mean-square force of 0.0003 a.u. No symmetry restrictions were imposed during the optimization. In all these DFT computations we used the Gaussian-09 program (Revision A.01).

Acknowledgement. We thank G. Shi and B. Zhu for constructive suggestions.

References

[1] Griffith K J *et al.* 2018 *Nature* **559** 556
[2] Dunn B *et al.* 2011 *Science* **334** 928
[3] Bruce P G *et al.* 2012 *Nat. Mater.* **11** 19
[4] Li M *et al.* 2020 *Science* **367** 979
[5] Yang J *et al.* 2021 *Chin. Phys. Lett.* **38** 068201
[6] Zhao J *et al.* 2017 *Nat. Nanotechnol.* **12** 993
[7] Xiao L *et al.* 2017 *Nat. Energy* **2** 17119
[8] Kang B *et al.* 2009 *Nature* **458** 190
[9] Lin D *et al.* 2017 *Nat. Nanotechnol.* **12** 194
[10] Harper G *et al.* 2019 *Nature* **575** 75
[11] Razmjou A *et al.* 2019 *Nat. Commun.* **10** 5793
[12] Meshram P *et al.* 2014 *Hydrometallurgy* **150** 192
[13] Xing L *et al.* 2016 *J. Membr. Sci.* **520** 596
[14] Vikström H *et al.* 2013 *Appl. Energy* **110** 252
[15] Lu J *et al.* 2018 *Appl. Surf. Sci.* **427** 931
[16] An J W *et al.* 2012 *Hydrometallurgy* **117-118** 64
[17] Xiang W *et al.* 2017 *Hydrometallurgy* **171** 27
[18] Ferreira D A *et al.* 2009 *J. Power Sources* **187** 238
[19] Liu X *et al.* 2018 *Hydrometallurgy* **176** 73
[20] Zhi S *et al.* 2018 *Engineering* **4** 361
[21] Tran M K *et al.* 2019 *Nat. Energy* **4** 339
[22] Lang J *et al.* 2020 *Nat. Sustain.* **3** 386
[23] Lv W *et al.* 2018 *ACS Sustain. Chem. Eng.* **6** 1504
[24] Zhao G *et al.* 2020 *Adv. Mater.* **32** 1905756
[25] Yang H J *et al.* 2020 *Chin. Phys. Lett.* **37** 028103
[26] Shi G S *et al.* 2013 *Sci. Rep.* **3** 3436
[27] Geim A K and Novoselov K S 2007 *Nat. Mater.* **6** 183
[28] Tu Y S *et al.* 2020 *Chin. Phys. Lett.* **37** 066803
[29] Chen L *et al.* 2017 *Nature* **550** 380
[30] Shi G *et al.* 2018 *Nat. Chem.* **10** 776
[31] Joshi R K *et al.* 2014 *Science* **343** 752
[32] Zhang H *et al.* 2018 *Sci. Adv.* **4** eaaq0066
[33] Sahu S *et al.* 2019 *Sci. Adv.* **5** eaaw5478
[34] Cao Y *et al.* 2012 *Nano Lett.* **12** 3783
[35] Jeowski P *et al.* 2018 *Nat. Mater.* **17** 167
[36] Yang C *et al.* 2019 *Nature* **569** 245
[37] Bao W *et al.* 2014 *Nat. Commun.* **5** 4224
[38] Hummers W S *et al.* 1958 *J. Am. Chem. Soc.* **80** 1339
[39] Xu Y *et al.* 2008 *J. Am. Chem. Soc.* **130** 5856
[40] Pan D *et al.* 2009 *Chem. Mater.* **21** 3136
[41] Sun P *et al.* 2013 *ACS Nano* **7** 428
[42] Shi G *et al.* 2011 *Chin. Phys. B* **20** 068101
[43] Varma S *et al.* 2006 *Biophys. Chem.* **124** 192
[44] Tansel B *et al.* 2006 *Sep. Purif. Technol.* **51** 40
[45] Marcus Y 2009 *Chem. Rev.* **109** 1346
[46] Zhao Y *et al.* 2008 *Acc. Chem. Res.* **41** 157
[47] Zhao Y *et al.* 2008 *Theor. Chem. Acc.* **120** 215
[48] Schwarze M *et al.* 2019 *Nat. Mater.* **18** 242
[49] Yang Y *et al.* 2019 *Phys. Chem. Chem. Phys.* **21** 7623
[50] Sato H *et al.* 2018 *Sci. Rep.* **8** 2473
[51] Mu L *et al.* 2021 *Phys. Chem. Chem. Phys.* **23** 14662
[52] Zhao Y *et al.* 2011 *J. Chem. Theory Comput.* **7** 669
[53] Peng C Y *et al.* 1996 *J. Comput. Chem.* **17** 49

Supplementary Material for "**Selective Separation of Lithium Using Thermally Reduced Graphene Oxide Membranes"**

Context:

PS1: Experimental processes:
- **Experimental process for adsorption of salt solutions**
- **Experimental process for desorption of salt solutions**

PS2: Adsorption capacity of rGO membranes
PS3: Raman spectrometer spectra of rGO membranes
PS4: Reusability of rGO membranes

PS1: Experimental processes

• Experimental process for adsorption of salt solutions

Initial masses of dry rGO membranes were weighed~4mg. The freestanding rGO membranes were placed in the centre of the centrifuge tube to ensure its full exposure to added 30ml DI water or salt aqueous solutions. After immersion at room temperature for an hour, the free bulk solution was removed from the tubes, followed by centrifuging at 2000 rpm for 3 minutes to remove solutions on the surface of membranes. Salt solutions inside rGO membranes can be retained due to a strong capillary effect. At last, the membranes were dried at 60 ℃ for 12 hours. The masses of subsequent dry (the freestanding rGO membrane together with the inside salt) rGO membranes were weighed.

• Experimental process for desorption of salt solutions

The dry (the freestanding rGO membrane together with the inside salt rGO) membranes were placed in the centre of the centrifuge tube to ensure its full exposure to added 50ml HCl with concentration of 1 mmol/L. After immersion at room temperature for an hour, the free bulk solution was removed from the tubes, the concentrations of cations were determined using PS7800 inductively coupled plasma optical emission spectrometer (ICP-OES). Finally, we can obtain the absolute adsorption capacity of metal ions and the M/Li+ molar ratios in the rGO-140 membranes.

PS2: Adsorption capacity of rGO membranes

Upon increasing the reduction temperature from 100 ℃ to 140 ℃, the adsorption capacity of cations significantly decreases. Then, the adsorption capacity of cations slowly increases as the reduction temperature further increased from 140 ℃ to 180 ℃. The dependence of the adsorption capacity of cations on the

reduction temperature is quite similar to that of R_f/R_i. The rGO-140 membranes can absorb relatively fewer ions and have a higher selectivity for Li^+ over Mg^{2+}.

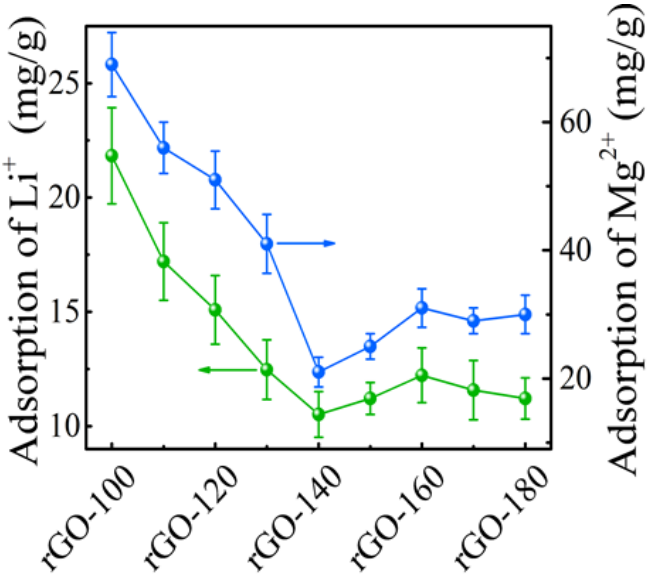

Figure S1: Adsorption capacity of rGO membranes for Mg^{2+} and Li^+, which immersed in solutions with a Mg^{2+}/Li^+ molar ratio of 1:1.

PS3: Raman spectrometer spectra of rGO membranes

Raman I_D/I_G ratios (where I_D and I_G are the D-band and G-band Raman intensities) are used to evaluate the defects of rGO membranes. As shown in Fig S1. a-b, the relative intensity (I_D/I_G) ratios of the D (~1,325 cm^{-1}) and G band (~1,590 cm^{-1}) for rGO membranes were 0.96, 0.99, 1.04, 1.03, 1.05, and 1.12, respectively. The I_D/I_G ratios became higher with increased reduction temperature, which shows that the defects of the rGO membranes are increased.

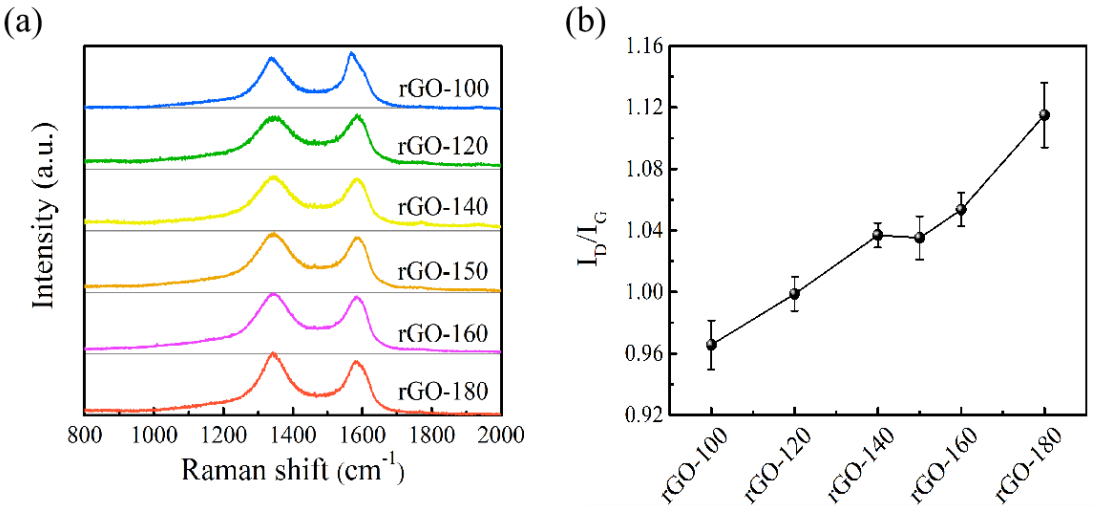

Figure S2: Characterizations of freestanding rGO membranes. (a) Raman spectra and **(b)** Raman I_D/I_G ratios, for the rGO membranes, which reduced at various temperatures. Error bars indicate the standard deviation.

PS4: Reusability of rGO membranes

In industrial applications, reusability is used to evaluate the feasibility of an adsorbent. Their reusability was investigated by adsorption and desorption experiment repeated for several times. After adsorption, the rGO membranes were desorbed by 1 mmol/L HCl, and then dried. The rGO membranes was then placed in a mixed Mg^{2+}/Li^{+} solutions. The adsorption capacity for Li^{+} decreased slightly with increasing treatment cycles, but remain 86.2% in the fifth cycle relative to the virgin one. After these cycles, the properties of the rGO membranes are still stable.

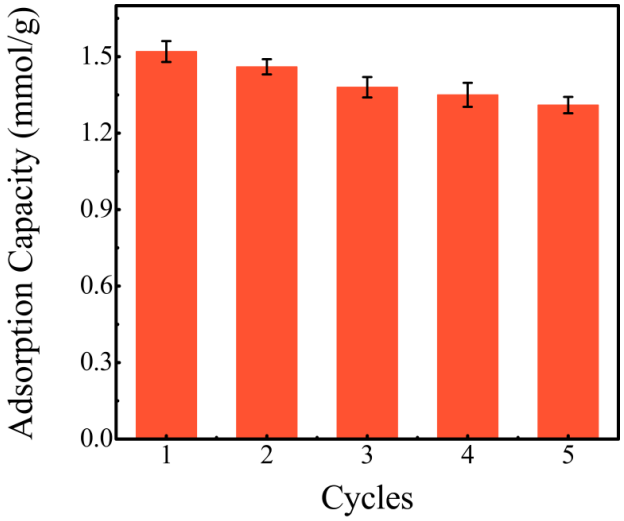

Figure S3: Recycling of rGO membranes for Li^{+} adsorption. Adsorption capacity with respect to the treatment cycles by rGO-140 membranes. Error bars indicate the standard deviation.